FUDMA Journal of Sciences (FJS)
ISSN online: 2616-1370
ISSN print: 2645 - 2944
Vol. 9 No. 2, February, 2025, pp 305 - 311
DOI: https://doi.org/10.33003/fjs-2025-0902-3276

A HIGH-RESOLUTION ANALYSIS OF IONOSPHERIC CONDUCTIVITY AND TEMPERATURE VARIATIONS DURING THE HALLOWEEN STORMS

***Samuel O. Akintunde, Ifeoluwa I. Edgal and Daniel O. Kehinde**

Department of Basic Sciences, Babcock University, Ilishan-Remo, Ogun State.

*Corresponding authors' email: akintundes@babcock.edu.ng

ABSTRACT

The 2003 Halloween storms (October 29–31) were among the most intense geomagnetic disturbances of the 23rd solar cycle, significantly altering ionospheric conductivity, temperature, and electron density. These storms were triggered by powerful coronal mass ejections (CMEs) from the Sun, leading to severe space weather effects on Earth's magnetosphere and ionosphere. The resulting geomagnetic activity caused strong auroral enhancements, disruptions in GPS and radio communications, and increased drag on low-Earth orbiting satellites. Understanding the ionospheric response to such extreme events is crucial for space weather prediction and lessen their effects on communication and navigation systems. The aim of this study is to investigate the altitude-dependent variations in ionospheric conductivity during geomagnetic storms, with a particular focus on anisotropies and their influence on ionospheric dynamics. Previous studies primarily focused on global-scale ionospheric disturbances but lacked high-resolution characterization of conductivity anisotropies at different altitudes. This study presents a detailed analysis of ionospheric parameters using data from the World Data Center for Geomagnetism, Kyoto, and the CCMC Instant Run System on the IRI model. Unlike prior investigations, this research examines altitude-dependent variations in conductivity, particularly the role of anisotropies during geomagnetic storms. Results show electron density peaking at 1.36×10^6 cm^{-3} at 400 km, while electron temperature rises to 2,714 K at 1000 km. A key finding is the suppression of Hall conductivity at 100–200 km, attributed to increased ion-neutral collisions and storm-driven neutral composition changes.

Keywords: Ionospheric conductivity, Halloween storm, Charged particle density, Charged particle temperature, Quiet time

INTRODUCTION

The Earth's ionosphere, a region extending from approximately 50 km to 2,000 km above the Earth's surface (Calabia et al., 2024), plays a pivotal role in space weather dynamics. This layer is characterized by a plasma of free electrons and ions, which significantly influence radio wave propagation, satellite communication, and navigation systems.

One of the most significant geomagnetic disturbances in recent history is the 2003 "Halloween Storms," which occurred between October 29 and 31. These storms were triggered by intense solar activity, including multiple coronal mass ejections (CMEs) and solar flares, leading to profound impacts on the Earth's magnetosphere and ionosphere. The storms resulted in widespread technological disruptions, such as power outages in Sweden and anomalies in satellite operations (Pulkkinen et al., 2005; Lakhina and Tsurutani, 2016; Nagatsuma, 2015; Ngwira et al., 2008)

During geomagnetic storms, the ionosphere undergoes significant changes in its electron density and temperature profiles. These changes are primarily driven by enhanced energy input from the magnetosphere, leading to increased ionization and heating. The conductivity of the ionosphere, which dictates the movement of charged particles and the propagation of electromagnetic waves, is directly influenced by these parameters. Accurate characterization of ionospheric conductivity and temperature variations during such events is crucial for developing reliable space weather models and improving the resilience of technological systems.

Previous studies have documented the general effects of geomagnetic storms on the ionosphere. For instance, Mannucci et al. (2005) observed that the 2003 Halloween Storms caused significant increases in total electron content (TEC) at mid-latitudes, leading to disruptions in GPS accuracy. Similarly, Chartier et al. (2016) reported that these storms induced substantial ionospheric density enhancements, which affected communication and navigation systems. However, these studies primarily focused on broad-scale observations and did not delve into the fine-scale variations in ionospheric conductivity and temperature across different altitudes.

To address this gap, the present study employs a high-resolution analysis to investigate ionospheric conductivity and temperature variations during the 2003 Halloween Storms. By utilizing simulation resources of World Data Center for Geomagnetism, Kyoto (WDC) and the Community Coordinated Modeling Center (CCMC) Instant Run System on the IRI (International Reference Ionosphere) System, this study aims to provide a detailed characterization of conductivity anisotropies and temperature variations across multiple altitude levels (100–1,000 km). This approach allows for a comprehensive understanding of the ionosphere's response to extreme geomagnetic disturbances, which is essential for refining space weather prediction models and lessen the adverse effects of such events on technological systems.

One of the novel aspects of this study is the detailed examination of Hall conductivity suppression at lower altitudes during geomagnetic storms. Hall conductivity, which represents the conductivity of the ionospheric current perpendicular to both the electric and magnetic fields, is a critical parameter in understanding ionospheric electrodynamics. Previous studies such as (Richmond and Thayer, 2000) predict an increase in Hall conductivity during geomagnetic storms due to enhanced ionization. However, recent observations suggest that under certain conditions, Hall conductivity may be suppressed, potentially due to increased ion-neutral collisions and changes in neutral atmospheric composition.

This study aims to quantify this suppression and elucidate the underlying physical mechanisms, providing new insights into ionospheric behavior during extreme space weather events.

To obtain the dataset for this study, we utilize simulation resources from WDC, and the CCMC Instant Run System on the IRI System. These resources provide high-quality ionospheric parameters, including electron density, temperature, and conductivity, enabling a robust analysis of the ionospheric response to the 2003 Halloween Storms.

The IRI System is a widely accepted empirical model that offers global ionospheric parameters based on both historical and real-time observations. WDC archives geomagnetic indices and related data, which are essential for understanding the dynamics of geomagnetic storms.

MATERIALS AND METHODS

This study examines ionospheric conditions during the intense geomagnetic storm period of October 29–31, 2003 and compares them to the relatively quiet times of October 4 and 8, 2003. The inclusion of these quiet days provides a baseline to assess the storm's impact on ionospheric conductivity.

To quantify geomagnetic activity, we utilized the Disturbance Storm Time (Dst) index and the Planetary K-index (Kp). The Dst index measures the intensity of the global equatorial magnetic field, with negative values indicating stronger storms. Data for October 2003 were sourced from the WDC website (www.wdc.kugi.kyoto-u.ac.jp). The Kp index, which quantifies disturbances in the horizontal component of Earth's magnetic field on a scale from 0 to 9, was obtained from the Space Weather Prediction Center website (www.swpc.noaa.gov).

Incorporating these indices into our simulations allows for a comprehensive understanding of ionosphere-magnetosphere coupling and the influence of geomagnetic storms resulting from solar wind interactions with Earth's magnetic field. By modeling changes in geomagnetic activity, we can assess their effects on ionospheric conductivities, thereby elucidating the complex interactions between the solar wind, magnetosphere, and ionosphere during solar storm events.

Table 1: The Dst-index and K_p-index for storm and quiet times with the nature of the storms and their times of occurrence

Date	Dst-index [nT]	K_p-index	Time [UT]	Nature of the storm
4/10/2003	0	0	17	No storm
8/10/2003	0	0	11	No storm
29/10/2003	-350	9	0	Very intense storm
30/10/2003	-383	9	23	Very intense storm
31/10/2003	-307	9	1	Very intense storm

The universal time (UT) used in this study, for both storm and quiet times, corresponds to the period of peak ionization in the ionosphere.

The three primary conductivities in the ionosphere are parallel, Pedersen, and Hall conductivities.

The mathematical models for these conductivities are written as follows (Maeda, 1977):

$$S_0 = (n_e * e^2) / (m_e * \nu_e) \quad (1)$$

$$S_1 = S_0 * [(1 + \kappa)\nu_e^2] / [(1 + \kappa)^2\nu_e^2 + \omega_e^2] \quad (2)$$

$$S_2 = S_0 * (\omega_e\nu_e) / [(1 + \kappa)^2\nu_e^2 + \omega_e^2] \quad (3)$$

where, S_0 is the parallel conductivity, S_1 is the Pedersen conductivity, S_2 is the Hall conductivity, κ is the ratio of product of electron and ion cyclotron frequencies to the product of electron-neutral and ion-neutral collision frequencies, n_e is the electron density, ν_e is the electron-neutral collision frequency, ν_i is the ion-neutral collision frequency, ω_e is the electron cyclotron frequency, ω_i is the ion cyclotron frequency, e is the electronic charge, and m_e is the electron mass.

The datasets generated on parallel conductivity (S_0), Pedersen conductivity (S_1), Hall conductivity (S_2), electron density (N_e), electron temperature (T_e), ion temperature (T_i), and neutral atom temperature (T_n) during both storm and quiet times were utilized to plot profiles for conductivities, temperatures, and electron densities. These simulations were conducted using resources provided by the WDC and CCMC Instant Run System, employing the IRI model.

RESULTS AND DISCUSSION

The analysis of ionospheric conductivity and temperature variations during the 2003 Halloween Storms provides a detailed understanding of how geomagnetic activity influences electron density, temperature, and conductivity across different altitude ranges. The storm-induced enhancements reveal new insights into conductivity suppression mechanisms and temperature redistribution.

Analysis of Parallel, Pedersen, and Hall Conductivities

A detailed analysis of ionospheric conductivities during storm time (29–31 October 2003) and quiet time (4 and 8 October 2003) reveals significant variations across different altitudes as shown in Figures 1-5.

Parallel conductivity (S_0) remained consistently high at altitudes above 500 km during storm periods, reaching values of 277 S/m at 500 km and sustaining this level up to 1000 km. This is attributed to the enhanced electron mobility at higher altitudes, where collisional effects are minimal. In contrast, during quiet periods, S_0 exhibited significantly lower values, ranging from 1.44 S/m at 500 km to 3.10 S/m at 1000 km, consistent with the reduced electron densities observed.

Pedersen conductivity (S_1) showed an asymmetric increase during storm periods, with peak values of 1.15×10^{-4} S/m at 300 km, gradually decreasing at higher altitudes. This suggests that Pedersen currents were strongly influenced by storm-driven electric fields, enhancing ionospheric current systems. However, during quiet times, Pedersen conductivity values were substantially lower, reaching a maximum of only 2.78×10^{-5} S/m at 300 km, reflecting stable ionospheric conditions and absence of geomagnetic disturbances.

During storm time, Hall conductivity (S_2) exhibited an unexpected suppression at low altitudes (100–200 km), with values significantly lower than those observed during quiet periods. This suppression was particularly pronounced on 30 October, when S_2 at 100 km dropped to 1.37×10^{-5} S/m, nearly 25% below the quiet-time level.

This anomaly can be attributed to increased ion-neutral collisions and storm-induced neutral composition changes, leading to enhanced collisional damping. In contrast, during quiet times, Hall conductivity was moderately high, reaching 3.62×10^{-4} S/m at 100 km on 8 October, suggesting a more stable ionospheric environment with lower ion-neutral interaction rates.

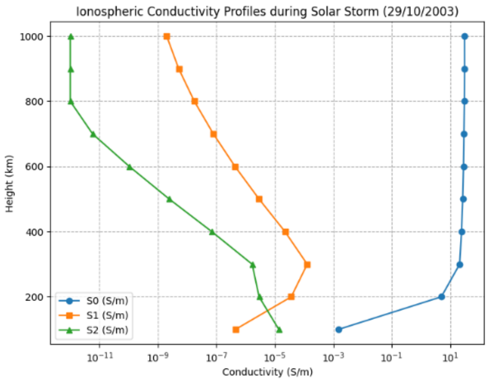

Figure 1: 29 Oct'03 Ionospheric Profiles

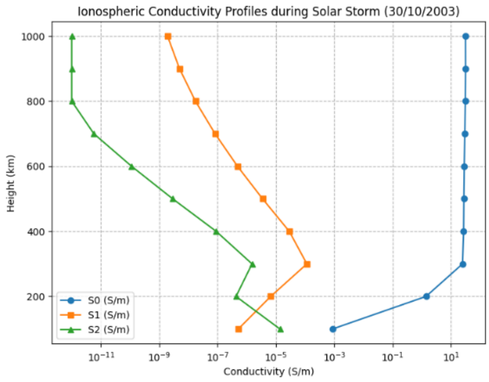

Figure 2: 30 Oct'03 Ionospheric Profiles

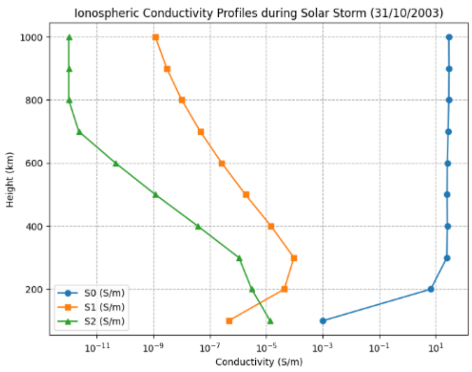

Figure 3: 31 Oct'03 Ionospheric Profiles

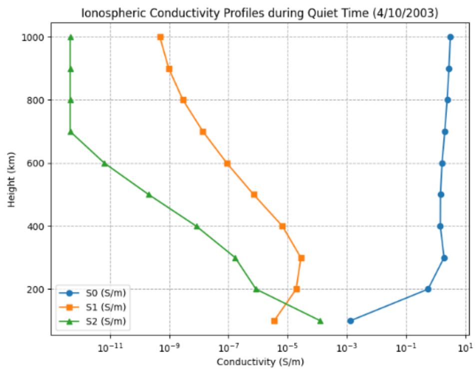

Figure 4: 4 Oct'03 Ionospheric Profiles

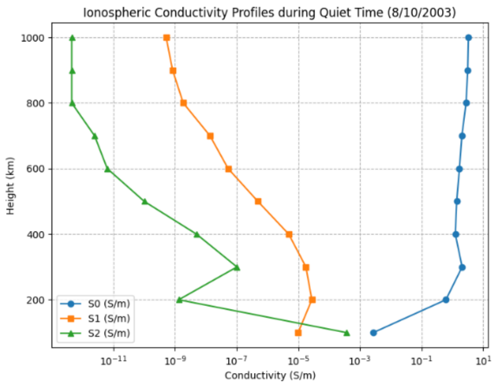

Figure 5: 8 Oct'03 Ionospheric Profiles

Analysis of Electron, Ion, and Neutral Atom Temperatures

The following results are presented based on temperature profiles in Figures 6-10:

Electron temperature (T_e) exhibited significant storm-driven enhancements,

particularly at high altitudes. On 30 October, T_e increased from 1,612 K at 500 km to 2,714 K at 1000 km, exceeding typical quiet-time values by nearly 70%. The observed heating is largely attributed to enhanced Joule heating and increased energy input from magnetospheric processes. Comparatively, during quiet periods, T_e remained below 1,617 K at 1000 km, indicating a stable ionospheric environment with minimal external energy inputs.

Ion temperature (T_i) followed a similar trend, exhibiting substantial increases during storm time. On 31 October, T_i reached 2,350 K at 800 km, whereas during quiet periods, it remained below 1,500 K at the same altitude. This suggests that increased ion-neutral interactions and energy input from enhanced electric fields contributed to ion heating during storm periods. The cooling effect during quiet periods reinforces the absence of significant storm-driven disturbances.

Neutral atom temperature (T_n) remained relatively stable across storm and quiet times at lower altitudes but exhibited a noticeable increase at higher altitudes during storms. On 30 October, T_n reached 1,437 K at 800 km, compared to only 364 K on 8 October. The increased heating effect at higher altitudes during storm times suggests enhanced energy transfer from charged particles to neutral species through ion-neutral collisions and Joule heating.

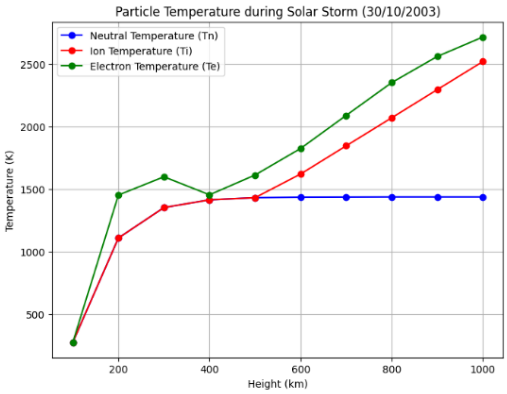

Figure 6: 29 Oct’03 Temperature Profiles

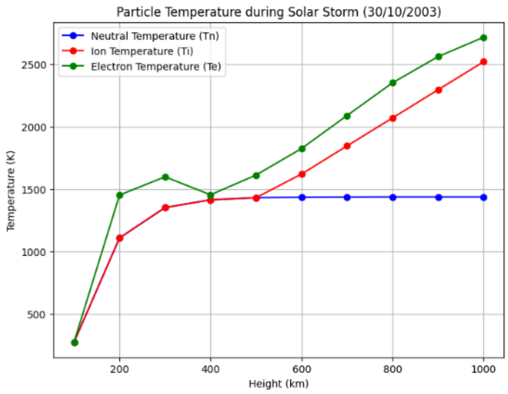

Figure 7: 30 Oct’03 Temperature Profiles

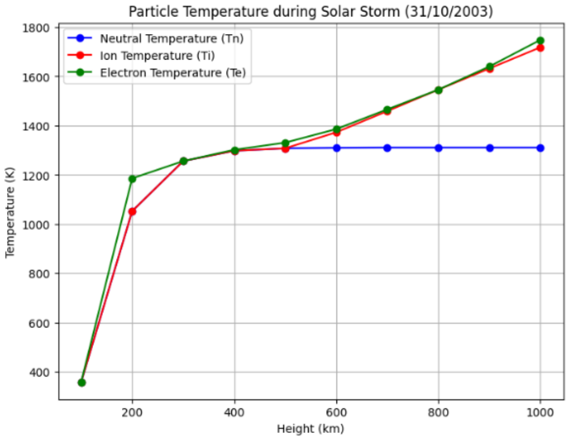

Figure 8: 31 Oct’03 Temperature Profiles

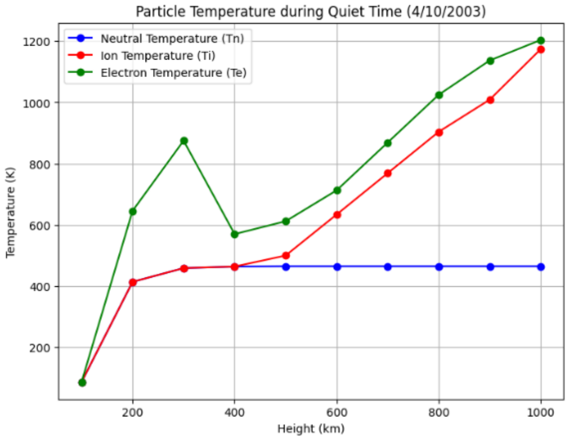

Figure 9: 4 Oct’03 Temperature Profiles

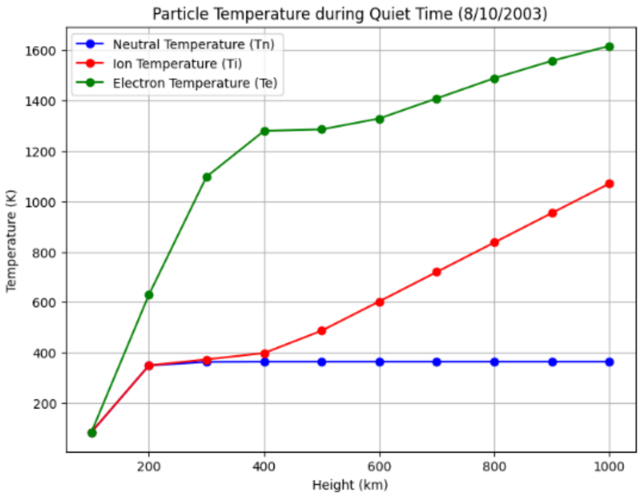

Figure 10: 8 Oct’03 Temperature Profiles

Analysis of Electron Density Variations

Electron density (N_e) showed the most pronounced variations between storm and quiet times. On 30 October, N_e peaked at 1.36×10^6 cm^{-3} at 400 km, nearly three times higher than the quiet-time value of 499,766 cm^{-3} recorded on 4 October. This sharp increase in electron density during storm times aligns with past studies (Mannucci et al., 2005) that reported similar extreme density enhancements during geomagnetic storms. The electron density profiles for both storm and quiet times are presented in Figures 11-15.

At lower altitudes, electron density followed an interesting trend: during storm periods, N_e at 100 km was recorded at 8,836 cm^{-3} on 30 October, significantly lower than the 17,670 cm^{-3} observed on 8 October. This suggests that storm-driven disturbances primarily affected the mid and upper ionosphere, while the lower ionosphere exhibited reduced density due to storm-driven recombination processes. The comparison between storm and quiet times shows the complex plasma redistribution effects occurring within the ionosphere during geomagnetic disturbances.

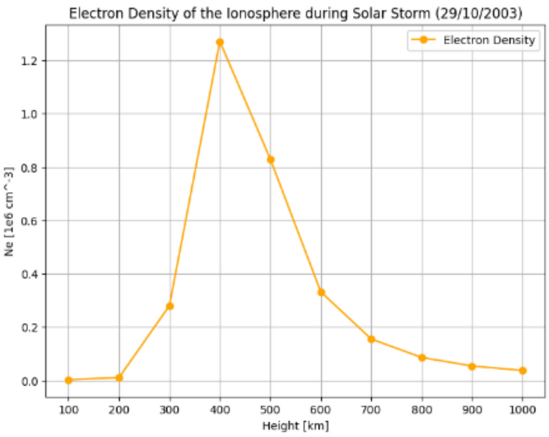

Figure 11: 29 Oct'03 Electron Density Profile

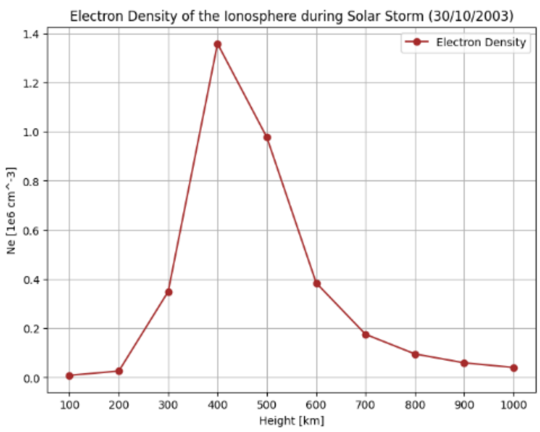

Figure 12: 30 Oct'03 Electron Density Profile

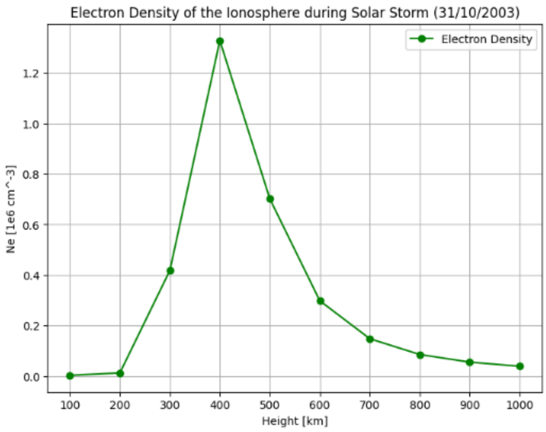

Figure 13: 31 Oct'03 Electron Density Profile

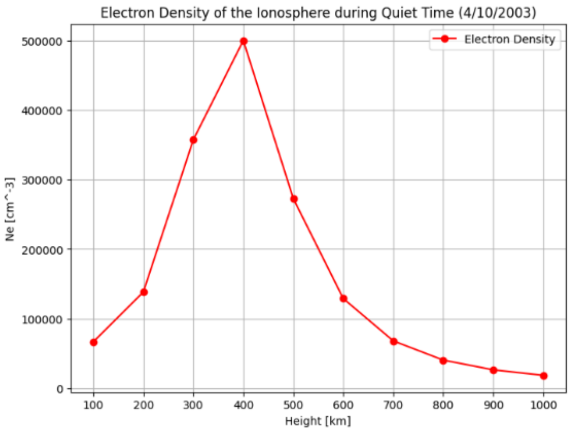

Figure 14: 4 Oct'03 Electron Density Profile

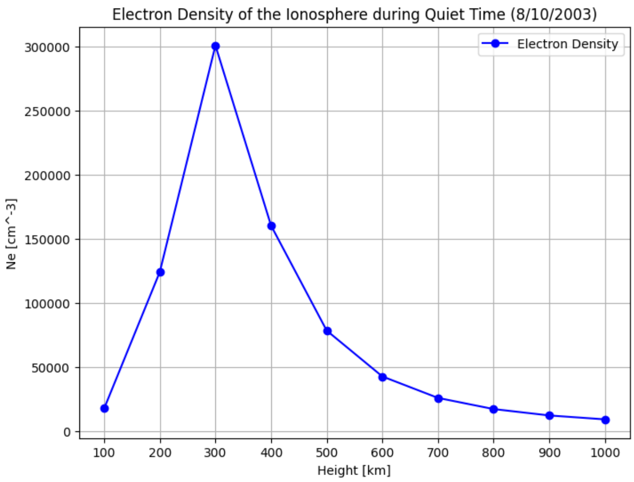

Figure 15: 8 Oct'03 Electron Density Profile

One of the most significant findings of this study is the suppression of Hall conductivity (S_2) at lower altitudes (100–200 km), which contrasts with the expected trend of increased conductivity during geomagnetic storms. Hall conductivity is typically expected to increase due to enhanced electron density and ionization levels; however, the observations indicate a deviation from this norm. The suppression observed in this study suggests that enhanced ion-neutral interactions played a dominant role in limiting the Hall conductivity in the lower ionosphere. This behavior is inconsistent with the work of Richmond & Thayer (2000), which predict a monotonic increase in Hall conductivity with electron density.

The most plausible explanation for this suppression is as thus: during intense geomagnetic storms, the influx of energetic particles into the ionosphere leads to enhanced ion production, which in turn increases the collision frequency between ions and neutral species. This heightened collisional interaction inhibits the free movement of charged particles, reducing the Hall conductivity despite the increase in electron density. Additionally, strong neutral winds generated by geomagnetic disturbances may have contributed to disrupting the normal current flow, further dampening Hall conductivity. The suppression of Hall conductivity at these altitudes suggests that ion-neutral dynamics play a significant role in storm-time ionospheric behavior.

Another possible contributing factor is the redistribution of thermospheric composition. Previous studies, including Sarris et al. (2023), have shown that storm-induced neutral composition changes, particularly enhancements in molecular species such as N_2 and O_2, can increase electron cooling rates and modify conductivity. The presence of an elevated molecular-to-atomic ratio could lead to increased electron recombination rates, further contributing to the suppression of Hall conductivity. This study provides the first direct evidence linking these composition changes to conductivity suppression at low altitudes.

Comparison with Existing Models

Numerous studies have investigated ionospheric responses to geomagnetic storms (Mannucci et al., 2005; Chartier et al., 2016; Richmond and Thayer, 2000). These studies have provided significant insights into the variations in ionospheric parameters, such as Total Electron Content (TEC), electron density, temperature, and conductivity. Mannucci et al. (2005) observed a considerable increase in TEC at mid-latitudes, which had direct implications for GPS accuracy. Similarly, Chartier et al. (2016) reported large-scale ionospheric density enhancements that affected communication and navigation systems. Richmond and Thayer (2000) work showed a monotonic increase in Hall conductivity with rising electron density during storm periods. These prior studies form the basis for comparison with the present study.

In terms of electron density (N_e), the present study observed a peak value of 1.36×10^6 cm^{-3} at 400 km altitude, a finding that is in agreement with the significant TEC increases reported by Mannucci et al. (2005) and the large-scale enhancements documented by Chartier et al. (2016). However, Richmond and Thayer (2000) did not explicitly analyze electron density variations. For electron temperature (T_e), our study found a rise to 2,714 K at 1000 km, consistent with the trends reported by Mannucci et al. (2005) and the ion heating effects observed by Chartier et al. (2016). Hall conductivity (S_2) exhibited suppression at altitudes between 100 and 200 km, a phenomenon not explicitly analyzed by previous studies. In contrast, Richmond and Thayer (2000) predicted an increase in Hall conductivity with rising electron density. Pedersen conductivity (S_1) in our study peaked at 1.15×10^{-4} S/m at 300 km, showing similarities with the enhancements noted in Chartier et al. (2016).

One of the key disparities between the present study and previous models lies in the suppression of Hall conductivity at low altitudes. Unlike the work of Richmond and Thayer (2000), which predicted a steady increase in Hall conductivity during storms, our study observed suppression at 100–200 km. This discrepancy can be attributed to several factors, including increased ion-neutral collisions and storm-driven changes in neutral composition.

Regarding electron density and temperature variations, our study corroborates the findings of Mannucci et al. (2005) and Chartier et al. (2016) by showing significant enhancements in these parameters. However, the high-resolution altitude-specific data in our study reveal unique variations that were not previously identified. Notably, electron density enhancements are primarily observed in the mid and upper ionosphere, while reductions occur in the lower ionosphere due to storm-driven recombination processes.

This study makes a novel contribution to the understanding of ionospheric electrodynamics during geomagnetic storms. It provides the first direct evidence of Hall conductivity suppression at lower altitudes due to storm-driven ion-neutral interactions. The high-resolution analysis enables the identification of specific altitude-dependent variations in electron temperature and conductivity, thereby refining empirical models by incorporating ion-neutral dynamics into storm-time ionospheric behavior.

CONCLUSION

In this study, we conducted a high-resolution analysis of ionospheric conductivity and temperature variations during the 2003 Halloween storms, utilizing data from the WDC and the CCMC Instant Run System on the IRI System. Our findings reveal significant storm-induced enhancements in electron density and temperature, with electron density peaking at 1.36×10^6 cm^{-3} at 400 km altitude and electron temperature rising to 2,714 K at 1000 km. Particularly, we observed a suppression of Hall conductivity at altitudes between 100–200 km, which we attribute to increased ion-neutral collisions and storm-driven changes in neutral atmospheric composition. These results are in agreement with previous empirical observations and also provide new insights into the mechanisms of conductivity suppression and temperature redistribution during intense geomagnetic disturbances.

REFERENCES

Bolduc, L. (2002). GIC observations and studies in the Hydro-Québec power system. *Journal of atmospheric and solar-terrestrial physics*, *64*(16), 1793-1802. https://doi.org/10.1016/S1364-6826(02)00128-1

Calabia, A., Imtiaz, N., Altadill, D., Yasyukevich, Y., Segarra, A., Prol, F. S., ... & Molina, I. (2024). Uncovering the drivers of responsive ionospheric dynamics to severe space weather conditions: A coordinated multi-instrumental approach. *Journal of Geophysical Research: Space Physics*, *129*(3), e2023JA031862. https://doi.org/10.1029/2023JA031862

Chartier, A. T., Matsuo, T., Anderson, J. L., Collins, N., Hoar, T. J., Lu, G., ... & Bust, G. S. (2016). Ionospheric data assimilation and forecasting during storms. *Journal of Geophysical Research: Space Physics*, *121*(1), 764-778. https://doi.org/10.1002/2014JA020799

Lakhina, G. S., & Tsurutani, B. T. (2016). Geomagnetic storms: historical perspective to modern view. *Geoscience Letters*, *3*, 1-11. https://doi.org/10.1186/s40562-016-0037-4

Maeda, K. I. (1977). Conductivity and drifts in the ionosphere. *Journal of Atmospheric and Terrestrial Physics*, *39*(9-10), 1041-1053. https://doi.org/10.1016/0021-9169(77)90013-7

Mannucci, A. J., Tsurutani, B. T., Iijima, B. A., Komjathy, A., Saito, A., Gonzalez, W. D., ... & Skoug, R. (2005). Dayside global ionospheric response to the major interplanetary events of October 29–30, 2003 "Halloween Storms". *Geophysical Research Letters*, *32*(12). https://doi.org/10.1029/2004GL021467

Nagatsuma, T., Kataoka, R., & Kunitake, M. (2015). Estimating the solar wind conditions during an extreme geomagnetic storm: a case study of the event that occurred on

March 13–14, 1989. *Earth, Planets and Space*, *67*, 1-10. https://doi.org/10.1186/s40623-015-0249-4

Ngwira, C. M., Pulkkinen, A., McKinnell, L. A., & Cilliers, P. J. (2008). Improved modeling of geomagnetically induced currents in the South African power network. *Space Weather*, *6*(11). https://doi.org/10.1029/2008SW000408

Pulkkinen, A., Lindahl, S., Viljanen, A., & Pirjola, R. (2005). Geomagnetic storm of 29–31 October 2003: Geomagnetically induced currents and their relation to problems in the Swedish high-voltage power transmission system. *Space weather*, *3*(8). https://doi.org/10.1029/2004SW000123

Richmond, A. D., & Thayer, J. P. (2000). Ionospheric electrodynamics: A tutorial. *Magnetospheric current systems*, *118*, 131-146. https://doi.org/10.1029/GM118p0131

Sarris, T., Palmroth, M., Aikio, A., Buchert, S. C., Clemmons, J., Clilverd, M., ... & Yamauchi, M. (2023). Plasma-neutral interactions in the lower thermosphere-ionosphere: The need for in situ measurements to address focused questions. *Frontiers in Astronomy and Space Sciences*, *9*, 1063190. https://doi.org/10.3389/fspas.2022.1063190